COMITATO NAZIONALE PER L'ENERGIA NUCLEARE
Laboratori Nazionali di Frascati

LNF-70/23
15 Maggio 1970

F. Felicetti : QED TESTS IN THE TIME-LIKE REGION. -

Servizio Documentazione
dei Laboratori Nazionali di Frascati del CNEN
Casella Postale 70 - Frascati (Roma)

Laboratori Nazionali di Frascati del CNEN
Servizio Documentazione

LNF-70/23

Nota interna: n. 479
15 Maggio 1970

F. Felicetti: QED TESTS IN THE TIME-LIKE REGION -

INTRODUCTION -

In the last few years several experiments have been performed in order to test the validity of quantum electrodynamics in the high energy region. Quantum electrodynamics is known to give an accurate description of electromagnetic interactions when momentum transfers which are small with respect to the particle rest masses are involved. It is not clear, however, whether the current formulation of quantum electrodynamics involving a renormalization procedure is a final theory or whether it is a particular solution to a more involved problem. This makes it important to verify, both in the time-like and space-like regions, the high energy behaviour of QED; that is, the photon, electron and muon description when these particles are very far off their mass-shell.

In this note I will be mainly concerned with QED tests in the time-like lepton region; space-like virtual lepton momenta will be briefly discussed since they are also involved in the current experiments testing the time-like virtual momentum region.

The first section is devoted to examining, in a very simplified form, in which direction and to what extent one can still expect a breakdown of the theory consistent with established experimental and theoretical results.

This section has of course no original content, in particular also review articles on this subject are already available[1, 2]; however, I have found it convenient to include it here in order to make this note self-consistent.

In section two some experimental tests of QED are discussed. The Frascati electron-proton wide angle bremsstrahlung experiment, testing time-like virtual lepton masses up to $(100\ \mathrm{MeV})^2$, is examined in detail. The radiative corrections problem is briefly outlined.

I - Quantum electrodynamics of a given set of spin 1/2 fermions (e, μ) describes the interaction of the electromagnetic field with the electron and muon field. Because of their interaction the electromagnetic and the fermion fields form a single dynamical system which must be described by a system of coupled equations. The equations of motion of quantum electrodynamics (QED).

$$(\not{p} + m)\psi = e\,\gamma_\mu A^\mu \psi \tag{1}$$

$$\Box A_\mu = -ie\bar{\psi}\gamma_\mu\psi \tag{2}$$

can be obtained from the variational principle $\delta \int L\, d^4x = 0$ with a Lagrangian density L

$$L = \bar{\psi}(\not{p} + m)\psi + F_{\mu\nu} F^{\mu\nu} + e\bar{\psi}\gamma_\mu\psi A^\mu$$

$$L = L_e + L_\gamma + L_{e\gamma} \tag{3}$$

$$F_{\mu\nu} = \partial_\nu A_\mu - \partial_\mu A_\nu \qquad j_\mu = ie\bar{\psi}\gamma_\mu\psi$$

where L_e, L_γ are the free field Lagrangian densities and $L_{e\gamma}$ is the term which describes the interaction.

In analogy with the classical case the vector j_μ eq. (3) is interpreted as the current generated by the particles and it can easily be shown that, owing to the Dirac equation, j_μ is a conserved current

$$\partial j_\mu = 0 \tag{4}$$

The Lagrangian density L eq. (3) is invariant under Lorentz transformations which follows directly from the fact that L is a scalar. L is in addition invariant under the gauge transformations

$$A_\mu \to A_\mu - \partial_\mu \phi$$

$$\psi \to \psi e^{-ie\phi} \tag{5}$$

where ϕ is any function whatever of the coordinates x, y, z, t which satisfies the equation $\Box\phi = 0$.

The requirement of invariance under gauge transformations corresponds to the classical fact that the physical meaning depends on the electric $\vec{E}$ and magnetic field $\vec{M}$ and not on the potential vector A_μ (*).

We note that the interaction term in the Lagrangian density (eq. 3) is the scalar product of the vector potential A_μ and the current density vector j_μ

$$L_{e\gamma} = j_\mu A^\mu \tag{6}$$

Therefore $L_{e\gamma}$ is linear in the potential A^μ, bilinear in the spinor field and does not contain derivatives of the fields.

This particular choice of the interaction term, which satisfies the general requirements of Lorentz and gauge invariance, is to some extent arbitrary and can only be justified by analogy with the classical case for a point-like particle where the interaction with the electromagnetic field can be introduced through the substitution

$$p \rightarrow p - eA \qquad \text{(minimal interaction)} \tag{7}$$

$L_{e\gamma}$ is indeed such that equation (1) for the interacting fields can be obtained from the Dirac equation for the free field by means of the minimal transformation of eq. (7).

The fact that $L_{e\gamma}$ is proportional to the electron charge and therefore the coupling constant of the electromagnetic interactions is of the order of 10^{-2} makes it possible to solve the equations of motion through perturbation techniques and leads to the introduction of the S-matrix formalism and Feynman diagrams.

In terms of Feynman graphs $L_{e\gamma}$ of eq. (6)implies that the lepton-

---

(*) - As is well known the existence of a conserved current and the gauge invariance of the Lagrangian density are strictly connected (Noether's theorem). If a Lagrangian density is invariant under gauge transformations of the first kind ($\psi \rightarrow \psi e^{i\phi}$ where ϕ is a constant) there exists a conserved current. If we have a Lagrangian density which is invariant under gauge transformations of the first kind, it is possible to construct a Lagrangian which is invariant under gauge transformations of the second kind ($\psi \rightarrow \psi e^{i\phi(x)}$) by the introduction of an interaction term $j_\mu A^\mu$ with a vector field which transforms as $A_\mu \rightarrow A_\mu - \partial_\mu\phi$. When we are dealing with gauge invariance of the electromagnetic Lagrangian density we are mainly concerned with gauge invariance of the second kind since in this way the interaction of the radiation field with a conserved current is automatically introduced.

-photon interaction is point-like and is described by the diagram of Fig. 1.

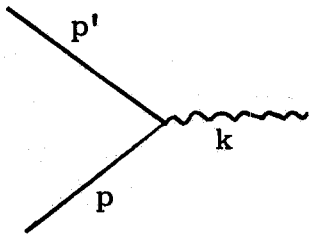

FIG. 1

This diagram describes the one-photon vertex related to the emission or absorption of a photon (four-momentum k) by the leptonic current.

Many photon diagrams such as shown in Fig. 2 do not enter in the current formulation of quantum electrodynamics.

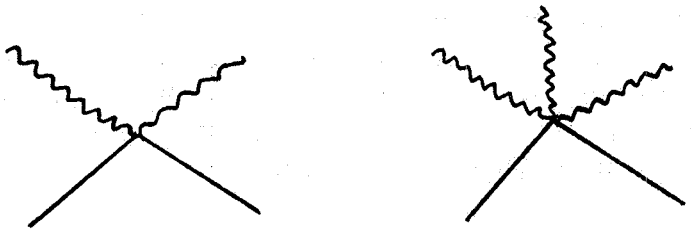

FIG. 2

From eq. (1) one has that each fermion propagator is given by

(8) $$S_F = \frac{\not{p} - m}{p^2 + m^2}$$

and the vertex function Γ_μ is given by

(9) $$\Gamma_\mu = \gamma_\mu$$

In this framework the photon propagator is given by $1/q^2$ (q is the four - momentum of the photon). We note that the fermion propagator (eq. 8) is determined by the free field Lagrangian L_e (eq. 3) and the vertex function is related to the current j_μ. Vertex functions and propagators, however, can be of a more general form.

Every modification of the current formulation of QED must correspond to a modification of the Lagrangian density $L \longrightarrow L'$ in such a way that L' is consistent with the general requirements of Lorentz and gauge invariance and that the new current j_μ is a conserved current. In terms of Feynman diagrams this corresponds to a modification of vertices and/or propagators.

The requirement that the current generated by the particles be a conserved current imposes, however, a connection between vertex function and propagators which is given by the Ward-Takahashi[4] identity

$$q_\mu \Gamma^\mu = S_F^{-1}(p') - S_F^{-1}(p) \tag{10}$$

where: $\Gamma^\mu(p, p', q)$ is the vertex function, S_F is the fermion propagator, $p(p')$ are the ingoing (outgoing) fermion momenta and $q = p'-p$.

Equation (10) evidently requires that any modification in the propagator be associated with some modification in the vertex function in order that current be conserved. The opposite, however, is not true: a vertex modification $\gamma_\mu \to \Gamma^\mu$ such that $q_\mu \Gamma^\mu = q_\mu \gamma^\mu$ does not require a propagator modification; vertex modifications of this kind are called intrinsic vertex modifications. Therefore the question of separating the effects induced on the vertex function by propagator modifications from those produced by intrinsic vertex modifications arises.

Drell and McClure[5] have been concerned with the vertex modifications associated with a generalization of the fermion propagator as constrained by the gauge invariance condition: in order to preserve gauge invariance the authors are required to introduce two-photon vertices. This is a consequence of the fact that the Ward-Takahashi identity takes account of only a small part of the restrictions imposed by current conservation; actually eq. (10) is a consequence of current conservation. The Ward-Takahashi identity is indeed a condition which is necessary but not sufficient. To guarantee the conservation of current in the general case the Chang-Mani[6] identities, which, actually, are a generalization of the Ward identity, must also be satisfied. The Chang-Mani identities in fact introduce in the theory the multiphoton vertices: the general statement is that one is required to associate with any propagator modification a certain number of multiphoton vertices, where the minimum number of multiphoton vertices required to guarantee the current conservation is immediately determined from the form of the modified propagator.

At this stage, however, the theory does not give a standard construction for the multiphoton vertices. This situation is very similar to that which we meet even in the standard formulation of quantum electrodynamics: that is, the standard propagator imposes only some restrictions upon the form of the vertex function which one could introduce (i.e., the form of the interaction Lagrangian density $L_{e\gamma}$) the actual form of the vertex function being determined by the additional requirement that the electromagnetic interaction be minimal (eq. 7). The implications of the Chang-Mani identities have been extensively treated by N. Kroll[7] who has given a construction scheme to deal with multiphoton vertices which relies on a generalization of the minimal electromagnetic interaction. In order to introduce Kroll's overall conclusions it is useful to discuss what can be the most general form of propagators and vertex functions.

A propagator modification corresponds to a modification of the free particle Lagrangian density L_e of eq. (3). The most general form of L_e which is consistent with Lorentz invariance has been studied by Lehman[8] and corresponds to a fermion propagator

$$S_F^{-1}(p) = A(p^2)\,\not{p} + B(p^2)m \tag{11}$$

where $A(p^2)$ and $B(p^2)$ are functions of the invariant p^2 such that

$$\left.\begin{matrix} A(p^2) \\ B(p^2) \end{matrix}\right\} \longrightarrow 1 \qquad \text{as } p^2 \longrightarrow m^2 \tag{12}$$

Equation (12) accounts for the fact that we require that $S_F^{-1}(p, m)\psi = 0$ represent the equation for the free particle as $p^2 \longrightarrow m^2$.

From the Chang-Mani identities one easily has that if $S_F^{-1}(p)$ is a polynomial in p of degree n, then multiphoton vertices up to and including rank n are required to restore current conservation.

Kroll has shown that it is possible to generalize the notion of minimal electromagnetic interaction (eq. 7) in such a way that the modifications induced by the propagator into the current and therefore into the vertex do not contain any intrinsic part. As a consequence the striking result obtained by Kroll is that the effect of a propagator modification cancels out the effect of vertex modifications induced by the Ward-Takahashi identity (i.e. non intrinsic vertex modifications) + the effect of induced multiphoton vertices. That is to say, a theory built with a modified propagator is completely equivalent to the current formulation of quantum electrodynamics.

Kroll's result holds for Feynman diagrams with open fermion lines; it is no longer true when closed loops are considered. In this particular case, however, the effects of fermion propagator modifications can not be experimentally checked as they are indistinguishable, in lowest order in e^2, from the effects of photon propagator modifications. Therefore the only modifications of the theory which can be experimentally checked with cross sections measurements are, at present, vertex function modifications.

Having dealt with the problem of propagator modifications let us now consider vertex functions.

The most general form for the electromagnetic vertex when all the three particles of the diagram of Fig. 1 are off the mass-shell is[9]

$$\Gamma_\mu(p, p', q) = \sum_{i,k}^{0.1} (\not{p}' + m)^i \left\{ G_1^{ik}\gamma_\mu + G_2^{ik}\sigma_{\mu\nu}q^\nu + G_3^{ik}q_\mu \right\} (\not{p} + m)^k \tag{13}$$

where the G_r^{ik} are twelve arbitrary functions of the invariants p^2, p'^2, $q^2 = (p' - p)^2$. Charge conjugation invariance requires

$$G_r^{ik} = (-1)^n G_r^{ki} \begin{cases} n = 0 & r = 1, 2 \\ n = 1 & r = 3 \end{cases}$$

so that eq. (13) involves only nine form factors. We note that the form factors G_2^{ik} correspond to intrinsic vertex modifications since $q_\mu \sigma_{\mu\nu} q^\nu = 0$. In the case $G_3^{ik} \neq 0$ then we have $q^\mu \Gamma_\mu \neq q^\mu \gamma_\mu$. That is to say, the vertex modifications induced by the G_3^{ik} are not intrinsic vertex modifications; they require, therefore, a propagator modification and the introduction of the induced multiphoton vertices. The effect of these vertex modifications is still contained in the general result obtained by Kroll so that the overall effect of the G_3^{ik} functions is negligible from an experimental point of view.

We can therefore put $G_3^{ik} = 0$ so that the general form for the electromagnetic vertex contains only six form factors which are connected with intrinsic vertex modifications. The effect of these six form factors can be separately investigated making use of the fact that they are all effective only when all the three particles of Fig. 1 are off the mass-shell.

When the ingoing (outgoing) fermion is on the mass-shell the form factors $G_{1,2}^{ik}$ corresponding to k = 1 (i = 1) do not enter since

$$(\not{p} + m)\,\Psi = 0 \qquad\qquad (\not{p}' + m)\,\Psi = 0$$

and the vertex function contains only four form factors. If both fermions are on the mass-shell only the form factors G_1^{00} and G_2^{00} are effective and the vertex Γ_μ may be written in the form

$$\Gamma_\mu = G_1^{00}(q^2)\,\gamma_\mu + G_2^{00}(q^2)\,\sigma_{\mu\nu} q^\nu \tag{14}$$

According to the preceding discussion we can conclude that the validity of the current formulation of quantum electrodynamics can be analized in terms of form factors of the vertex function. This corresponds to the possibility that the electron and the μ meson do not behave like point-particles; that is, they have structure which must be described by form factors which, when the particles are on the mass-shell, reduce to the electric and magnetic form factors. This is completely analogous to what one does for protons, the structure of which is expressed by the vertex function Γ_μ of eq. (14) with

$$G_1^{00} = e\,F_1(q^2) \qquad\qquad G_2^{00} = e\,\frac{K}{M}\,F_2(q^2)$$

(K anomalous magnetic moment, M mass of the proton).

The problem of modifying quantum electrodynamics for photons has been extensively investigated in connection with the divergence difficulties that the theory shows when, as an example, one is dealing with the electromagnetic mass differences between hadrons in the same isospin multiplet.

The divergence difficulties in electrodynamics, which are connected to the form of the photon propagator $1/q^2$, can be simply removed assuming the existence of a "heavy photon" with mass M and thus writing for the photon a regularized propagator

$$\frac{1}{q^2} - \frac{1}{q^2 + M^2} \tag{15}$$

This means a well defined modification of the interaction Lagrangian $L_{e\gamma} = j_\mu A^\mu$. In order to obtain the second term in the modified propagator (15), one has to introduce a neutral massive spin 1 boson field B_μ with an interaction

$$i\, j_\mu B^\mu$$

The complete interaction Lagrangian density that one gets is therefore

$$L'_{e\gamma} = j_\mu (A^\mu + i B^\mu)$$

which is, however, no longer hermitian $L'_{e\gamma} \neq L'^{+}_{e\gamma}$.

The difficulties arising out of a non-hermitian Lagrangian density have been recently discussed by T.D. Lee and G.C. Wich[10] who have shown however the possibility of a consistent formulation of the theory: in particular they have demonstrated that the unitarity of the S-matrix can be preserved.

Here we will only note that the regularized propagator of eq. (15) has some well defined experimental implications: if one considers the second term in the propagator (15) as the propagator of a "heavy photon" the pole of this particle is on the physical sheet of the complex energy plane. The experimental implications of this modified propagator are discussed in reference (11). With colliding beams experiments, such as $e^+ + e^- \rightarrow e^+ + e^-$ and $e^+ + e^- \rightarrow \mu^+ + \mu^-$, we can test both the existence of a "heavy photon" with mass M and the sign of the second term in the regularized propagator (15). At present the experimental limit on M is $M > 3.3$ GeV.

II. - EXPERIMENTAL QED TESTS. -

When we are dealing with electromagnetic reactions at least one of the interacting particles can be virtual. We say that we are testing QED

in the high energy region when the modulus of the squared four-momentum of the virtual particle is large compared to the squared electron mass.

The validity of quantum electrodynamics in the high energy region can be verified both with measurements of static properties like the g-2 factor of electron and muon and in dynamical tests like the determination of cross sections of genuine electromagnetic processes.

Present techniques allow the measurement of static properties to better than some parts to 10^{-7} accuracy; the measurement of cross sections to a few percent. Both kind of measurements, however, are relevant since they represent complementary and independent tests of the theory. When measuring static properties, high order processes give the relevant contributions with large virtual momenta appearing in loop diagrams (Fig. 3) (i.e. as a part of an integration range extending from the mass shell to infinity). In dynamical tests, however, it is possible to select by kinematics sharply defined virtual momenta. That is to say, cross section measurements allow one to test quantum electrodynamics as a function of the energy.

The measurement of the g-2 factor of charged leptons is one of the most refined static QED tests. The gyromagnetic factor, g, of the electron and muon is not expected to be exactly 2 by QED, although no magnetic moment term appears in the current (eq. 3), because of higher order corrections from graphs like the one of Fig. 3.

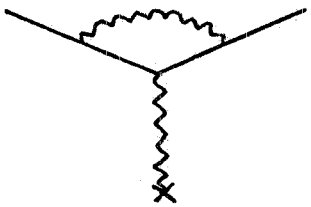

FIG. 3

The g-2 factor calculation involves photon and lepton propagators as well as the electromagnetic vertex when two lines, one photon and one lepton, are far off their mass shells. In this case large virtual momenta contribute through the loop integration. This measurement is then sensitive to a form factor in the lepton photon vertex and to the behaviour of the photon propagator.

Experiments and theory give results in good agreement[12]

	$\left\{\frac{g-2}{2}\right\}_{\text{experiment}}$	$\left\{\frac{g-2}{2}\right\}_{\text{theory}}$
e	$(115956 \pm 3)\ 10^{-8}$	$(115964 \pm .4)\ 10^{-8}$
μ	$(116616 \pm 31)\ 10^{-8}$	$(116560)\ 10^{-8}$

which excludes, within the limits of experimental and theoretical accuracies, a magnetic form factor in the lepton photon vertex.

As far as concerns the vertex function of eq. (13) this means that we can set $G_2^{00} = 0$ since $G_2^{00}(0)$ represents, to order zero, the anomalous

magnetic moment of the involved lepton. In addition, since the g-2 experimental value agrees well with the theoretical one evaluated to higher order with QED (where one assumes point-like electron and Dirac propagator) one can infer than, apart from improbable cancellations because of the loop integration, all the functions G's of eq. (13) are consistent with QED predictions.

As long as one wishes to do no more than parametrize the degree to which the theory has been experimentally confirmed, the introduction of particular models of breakdown [like the usual hypothesis of an electric form factor $F(q^2) = (1 + q^2/\Lambda^2)^{-1}$] allows one to put in a quantitative way the limits to which the theory has been checked. The limits on Λ^2 that one gets from the g-2 experiment are of the same order of magnitude of those which can be obtained from high energy experiments.

Dynamical QED tests can be classified according to the Feynman diagram which is relevant in the first order description of the process. This allows us to immediately recognize the kind of test which is connected to the studied reaction. To the first order, three distinct kind of diagram can occur depending on the specific nature of involved particles:

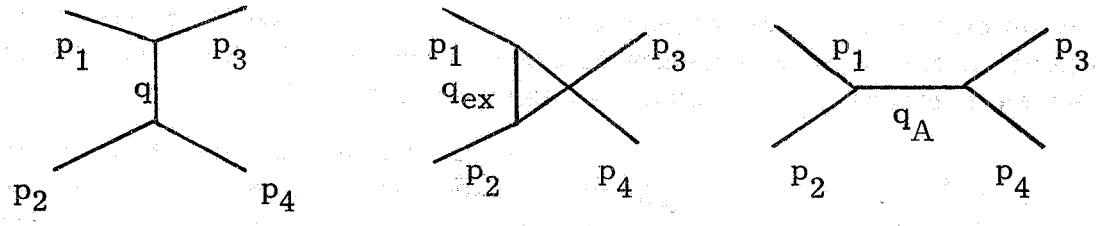

$q^2 = (p_3 - p_1)^2$ $\qquad$ $q_{ex}^2 = (p_4 - p_1)^2$ $\qquad$ $q_A^2 = (p_1 + p_2)^2$

FIG. 4

In general every process is described by two of these diagrams together. When dealing with scattering and exchange diagrams space-like momenta are involved ($q^2, q_{ex}^2 < 0$) whereas time-like momenta occur in the annihilation diagram ($q_A^2 > 0$).

In the center of mass system the entire four-momentum of reacting particles can be put into the virtual intermediate states; this makes the center of mass a highly privileged system. Storage rings which allow one to work in the center of mass will give then one of the best possibilities of testing QED.

Storage rings experiments from the point of view of QED have been extensively discussed by R. Gatto[13]. Currently this technique is

limited to e^-e^- and e^+e^- collisions; thus, the reactions to be considered in the realm of storage rings are, at present

I) $e^- + e^- \rightarrow e^- + e^-$

II) $e^+ + e^- \rightarrow e^+ + e^-$

III) $e^+ + e^- \rightarrow \mu^+ + \mu^-$

IV) $e^+ + e^- \rightarrow \gamma + \gamma$

This allows one to study photon propagator both in the time-like and space-like region as well as the lepton photon vertex. At present e^-e^- scattering has been measured at Stanford by the Princeton-Stanford group[14] testing space like photon propagators up to 2 x 550 MeV. The measured angular distribution is in good agreement with QED prediction but no absolute normalization has been checked. Also, large angle elastic e^+e^- scattering has been measured at the storage ring ACO (Orsay) probing mainly space-like virtual photons up to 2 x 510 MeV total center of mass energy[15]. Absolute measurements have been done in this case, and the agreement between theory and experiment is very good. An experiment on $e^+e^- \rightarrow \mu^+ + \mu^-$ is actually in progress at the Frascati storage ring Adone so that results on the time-like photon propagator will be available very soon.

SPACE-LIKE LEPTONS -

The annihilation of electron pairs into 2 photons ($e^+ + e^- \rightarrow \gamma + \gamma$) would provide a clean test of electron photon vertex at space-like lepton four-momenta (Fig. 5). An experiment of this kind, which measures the angular distribution of the produced γ rays as a function of the total c.m. energy, is sufficient to study the e γ e vertex and no absolute cross section measurement is needed.

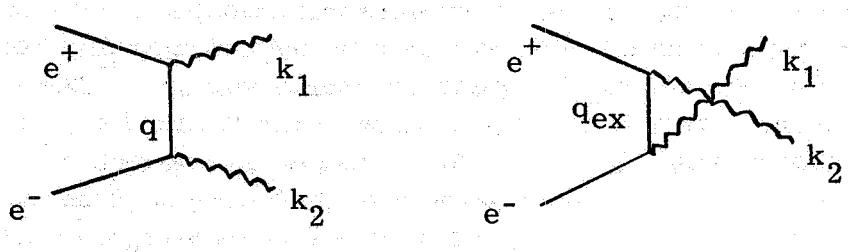

FIG. 5

A measurement of the total cross section of this process has been done using fast positrons on atomic electrons at rest[16]; virtual lepton momenta that one gets in this way, however, are quite small even for very high energies of the ingoing positrons.

At present, an experiment on 2 γ annihilation is in progress at the storage ring Adone[17]; in this case, due to the coincidence of center of mass and laboratory systems, high space-like lepton four momenta ($\sim$2 GeV) and a very clean test of QED can be obtained.

Till now, space like leptons have been studied in $e^+e^-(\mu^+\mu^-)$ pair-photoproduction experiments mainly on carbon nuclei. This kind of processes differ from the 2 γ annihilation only in the fact that one of the photons is virtual and ends on strongly interacting particles (Fig. 6a).

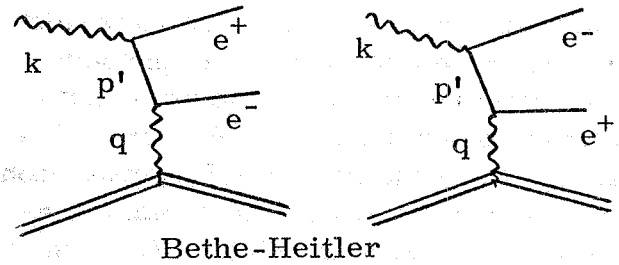

Bethe-Heitler
FIG. 6a

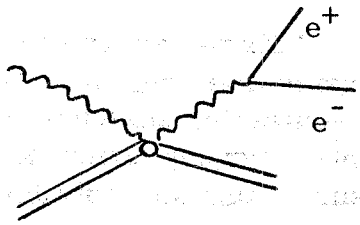

Virtual Compton
FIG. 6b

The presence of a nucleus as a target introduces in this kind of experiment the contamination due to the strong interactions like the Virtual Compton contribution shown in Fig. 6b; in addition corrections for the form factor of the target nucleus are required.

The four-momentum of the virtual lepton p' in the two Bethe-Heitler diagrams is given by

$$p'^2 = (k - p^{\pm})^2 \simeq - 2kp^{\pm}(1-\cos\theta^{\pm})$$

so that p'^2 is uniquely determined by the apparatus only for symmetric pairs; in this case $p'^2 \simeq -k^2\theta^2/2$. In addition, the symmetric arrangement allows one to keep the four momentum of the virtual photon q^2 as low as possible in order to minimize the nuclear recoil and thus the correction for the nuclear form factors.

Another advantage of the symmetric condition (both in spatial momenta and in the leptonic charges) is that the interference term between Bethe-Heitler and virtual Compton diagrams vanishes, due to the different transformation properties under charge conjugation of this two contributions, so that virtual Compton contamination is reduced to the order of a percent. In general, virtual Compton contributions and the inelastic nuclear form factors introduce uncertainties of some percent in the interpretation of wide angle pairs photoproduction as genuine QED processes.

We next consider another source of contamination which is present when the invariant mass $M^2 = (p^+ + p^-)^2$ of the produced lepton pair approaches the $\jmath^o$ mass; in this case the $\jmath^o$ photoproduction and their subsequent decay into $e^+e^-(\mu^+\mu^-)$ pairs give a relevant contribution to

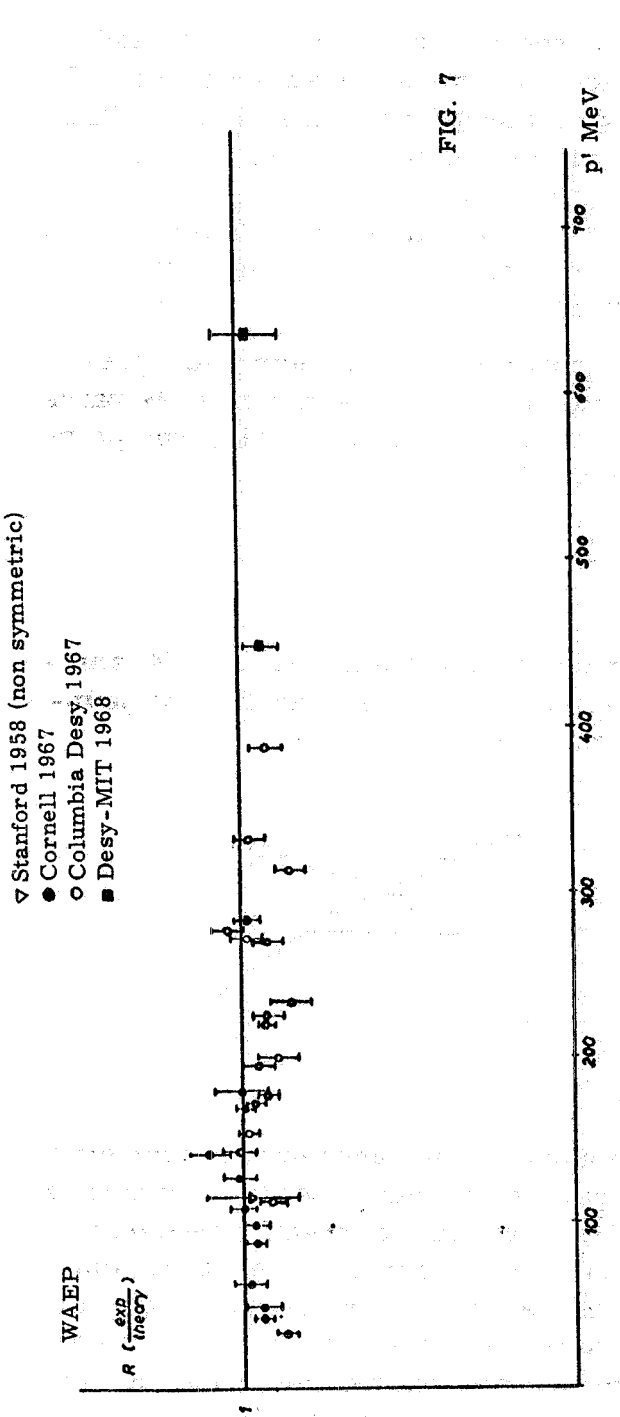
WAEP
R (exp/theory)
▽ Stanford 1958 (non symmetric)
● Cornell 1967
○ Columbia Desy 1967
■ Desy-MIT 1968
1
100
200
300
400
500
600
700
p' MeV

FIG. 7

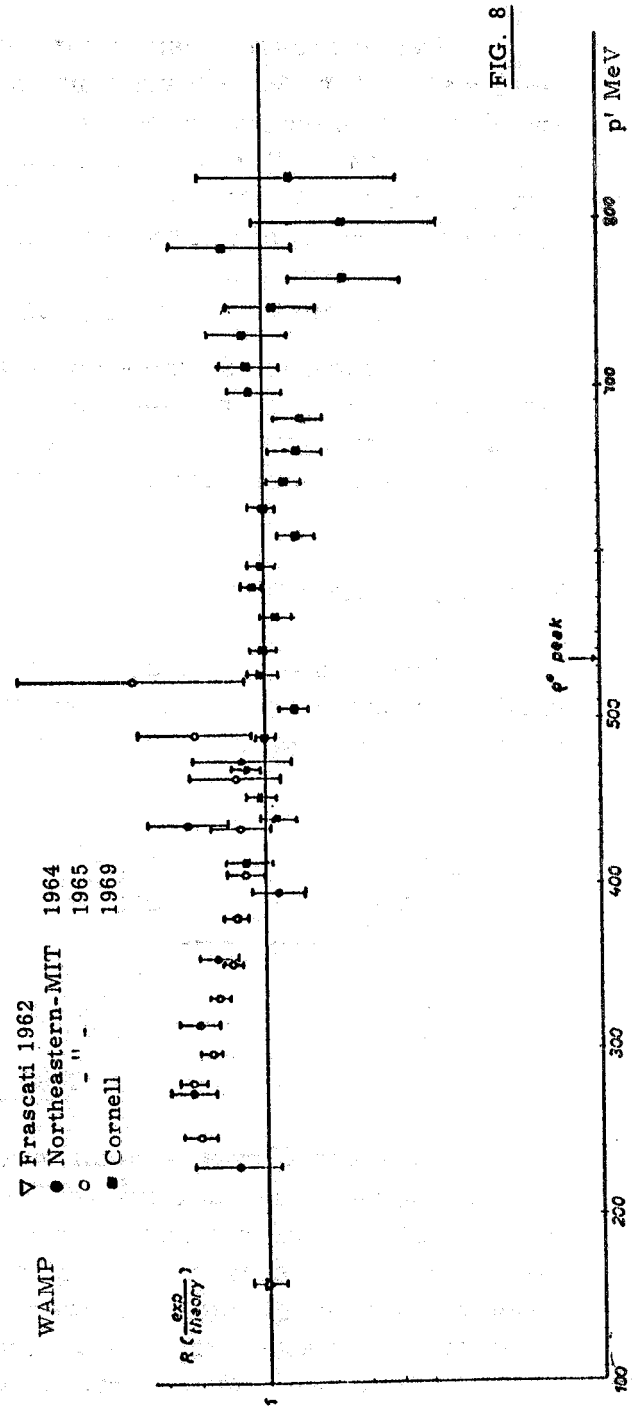
WAMP
R (exp/theory)
▽ Frascati 1962
● Northeastern-MIT 1964
○ " " 1965
■ Cornell 1969
ρ° peak
1
100
200
300
400
500
600
700
p' MeV

FIG. 8

the pair photoproduction cross section. The two processes can however be distinguished to some extent owing to the fact that the pair aperture angle distribution is quite different in the Bethe-Heitler and ϱ^0 contributions.

Experimental results for symmetric electron (WAEP)[18] and muon pairs (WAMP)[19] photoproduction on carbon are shown in Fig. 7 and Fig. 8 respectively; the ratio R of measured cross sections to QED predictions is plotted as a function of the four momentum of the virtual lepton p' up to $|p'| \sim 800$ MeV. The errors shown in Figs. 7, 8 are essentially an estimate of systematic effects such as virtual Compton contribution, radiative corrections and ϱ^0 photoproduction, the last of which is relevant only for $|p'| \gtrsim 400$ MeV.

The measured cross sections appear to be in substantial agreement with QED predictions; the same applies to the asymmetric μ pairs measurement (Quinn-Ritson) and to the recent symmetric electron pairs photoproduction experiment on hydrogen[18].

TIME LIKE LEPTONS. -

The Compton effect $e + \gamma \rightarrow e + \gamma$ is the analogue of 2γ annihilation of pairs in the time-like region and is the best reaction in principle to study the $e\gamma e$ vertex with time-like electrons (Fig. 9).

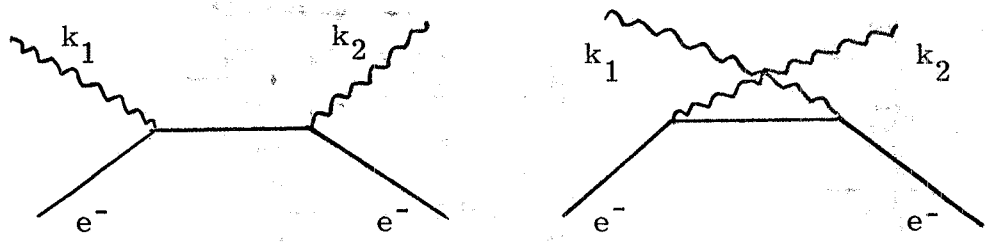

FIG. 9

Although Compton scattering has the advantage that no strongly interacting particles are present to confuse the test, serious experimental difficulties would arise from the fact that the kinematic situation in the laboratory system is very poor. In order to get high virtual lepton momenta very high energy photons are needed; even with 20 GeV photons, however, the maximum virtual momentum one gets is only of the order of 100 MeV/c. In addition most of the relevant events are produced, in the laboratory system, with very small scattering angles (some 10^{-3} rad typically).

A way out is to allow for the presence of a massive body as a target of virtual photons to which a large fraction of the ingoing momen

tum can be transferred. This process, of course, is seen as wide angle bremsstrahlung which is, at present, the most useful reaction to test QED in the time-like region.

Electron proton bremsstrahlung is described to the lowest order in e^2 by the two Bethe-Heitler diagrams (Fig. 10a).

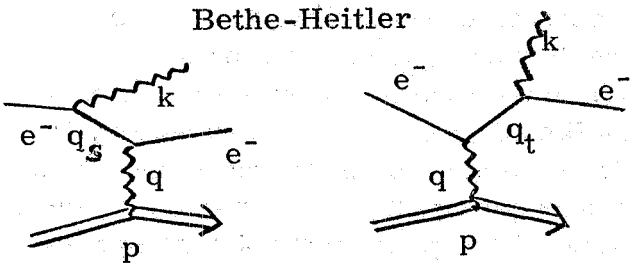

FIG. 10 a)

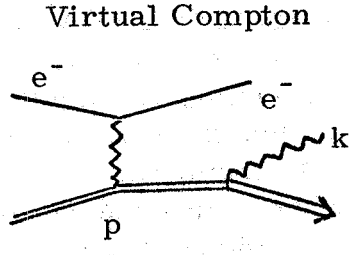

FIG. 10 b)

and differs from the Compton scattering only in the fact that one of the photons is virtual and interacts with a proton. The $p\gamma p$ vertex, however, is well known from electron-proton scattering so that one can proceed to calculate the Bethe-Heitler cross section (Fig. 10a) accounting for the effects of hadron physics in terms of the two electric and magnetic form factors of the proton $F_1(q^2)$ and $F_2(q^2)$ - (q^2 four-momentum of the virtual photon).

Besides the dominant Bethe-Heitler diagrams (Fig. 10a) also the virtual Compton effect contributes to the bremsstrahlung cross section (Fig. 10b). In this case the interference term between virtual Compton and Bethe-Heitler diagrams does not vanish so that a more accurate evaluation of the virtual Compton contribution, as compared to symmetric pairs photoproduction experiments, is needed.

Electron-proton bremsstrahlung experiments have been undertaken in various laboratories following a suggestion by F. Low[20] of a simple violation of standard QED due to the existence of a "heavy electron" e^* rapidly decaying into $e + \gamma$

$$e + p \longrightarrow e^* + p$$
$$\hookrightarrow e + \gamma$$

This kind of experiment, which represents the test of a particular model of QED breakdown, is a simplified versions of WAB relying on the search for the elastic production peak in the recoil proton energy spectrum that should accompany the production of a real, though unstable, particle. Till now no evidence has been found for a heavy electron having a mass less than 1.3 GeV[21].

Absolute measurements of electron-proton bremsstrahlung cross

section, as the one I will discuss in the following, have instead the advantage of providing model independent QED tests in the time-like region.

Recently performed experiments on electrons and muons bremsstrahlung on carbon nuclei[22, 23] did explore the lepton-photon vertex up to time-like virtual lepton masses of ~ 1.2 GeV. The agreement with QED predictions is good within the limits of experimental uncertainties ($\sim 15\%$). We note, however, that bremsstrahlung experiments on carbon are not completely equivalent to bremsstrahlung on hydrogen particularly as far as concerns the space-like momentum involved which, in the case of experiments on carbon, is in general of the same order of the time-like one. This makes this kind of experiment less sensitive to the time-like behaviour of the theory because of the presence of large space-like contributions. Results on electrons and muons bremsstrahlung are summarized in Fig. 14.

WIDE-ANGLE ELECTRON PROTON BREMSSTRAHLUNG -

In this section I will discuss the wide-angle electron-proton bremsstrahlung experiment which has been performed using the external electron beam of the Frascati 1 GeV Synchrotron by a Frascati-Napoli-Roma collaboration[24]. The differential cross section for wide angle electron-proton bremsstrahlung has been measured at two different values of the time-like virtual electron momentum q_t^2, keeping constant at the same time the space-like momentum q_s^2.

$$e + p \rightarrow e + p + \gamma$$

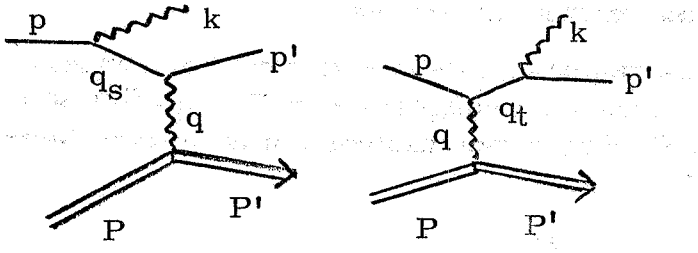

$q_t^2 = (70\ \text{MeV})^2 \quad q_s^2 = -(260\ \text{MeV})^2$

$q_t^2 = (100\ \text{MeV})^2 \quad q_s^2 = -(265\ \text{MeV})^2$

In order to have a continuous checking of the experimental apparatus the elastic electron-proton scattering cross section has also been measured in parallel to the WAB measurements; in addition, this can be used as a test of the quantamenter calibration.

With an incident beam intensity of 10^{10} electrons/sec typical counting rates were

WAB	~ 10 events/hour
elastic scattering	$\sim 10^5$ events/hour

The main contamination source to the bremsstrahlung measurement is the π^0 electroproduction which is characterized by counting rates of the same order of magnitude as the WAB.

The relevant features of wide angle bremsstrahlung are characterized by the invariants:

$$
\begin{aligned}
q_s^2 &= (p-k)^2 \simeq -2pk(1-\cos\theta_\gamma) \\
q_t^2 &= (p'+k)^2 \simeq 2p'k(1-\cos\theta_{e\gamma}) \qquad (16) \\
q^2 &= (P'-P)^2 = -2MT_p
\end{aligned}
$$

where p, p' and k are the four-momenta of the ingoing, outgoing electrons and photon respectively, θ_γ is the emission angle of the photon with respect to the line of flight of the ingoing electron, $\theta_{e\gamma}$ is the angle between the outgoing electron and photon; M and Tp are the proton mass and kinetic energy respectively.

The three outgoing particles (e, p, γ) were detected in coincidence. The experiment was run in such a kinematical configuration that electron and photon were detected when emitted at the same angle with respect to the incident beam, but symmetrically above and below the plane defined by the ingoing electron and the outgoing proton. This symmetric arrangement has the advantage of allowing one to change the relevant kinematical parameters orthogonally.

In particular in the symmetric situation, in which the energies of the electron and photon are equal, the time-like electron four-momentum q_t^2 is sharply defined by the angle between the emitted electron and photon $\theta_{e\gamma}$ and the space-like four-momentum q_s^2 is determined by the rotation angle of the electron and photon emission plane around their total three-momentum.

This allows one:

a) To change from one kinematical situation to the other, $q_t^2 = (70\ \text{MeV})^2 \rightarrow q_t^2 = (100\ \text{MeV})^2$ only by changing the detection angles of the electron and photon.

b) To fix q_t^2 quite independently of q_s^2 so that, as an example, one can keep q_s^2 constant and greater than q_t^2. When $-q_s^2 \gg q_t^2$, time-like momenta give the relevant contribution to the WAB cross section so that one can study the behaviour of the cross section as a function of q_t^2.

c) To keep constant the proton kinetic energy and thus the four-momentum q^2 of the virtual photon. As a consequence, the same proton form factors occur in the two kinematical conditions.

The layout of the experimental apparatus is shown in Fig. 11. The electron beam hits a 20 cm long liquid-hydrogen target which is enclosed in a magnet, not shown in figure, which produces a magnetic field ($\sim$ 400 Gauss) along the direction of incident electrons. This magnetic field was effective in sweeping out most of the soft electrons ($\sim$20 MeV)

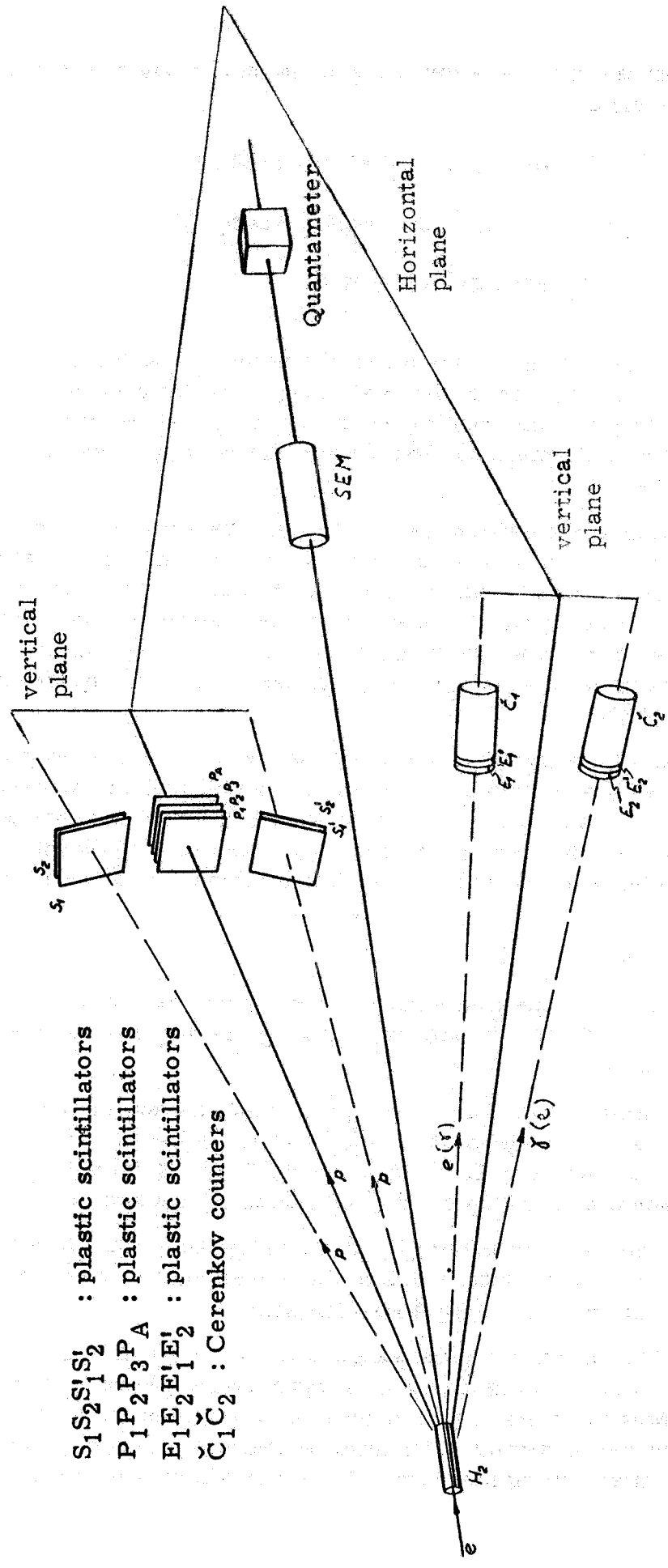

FIG.11 - Experimental apparatus. - $P_1P_2P_3P_A$ is the proton range telescope; $E_1E'_1\check{C}_1$, $E_2E'_2\check{C}_2$ (symmetrical with respect to the horizontal plane) are the electron and photon detectors; S_1S_2, $S'_1S'_2$ are the proton scattering telescopes; an e-p scattering event is defined by $(S_1S'_2)\cdot(E_1E'_1\check{C}_1)$ or $(S_1S_2)\cdot(E_2E'_2\check{C}_2)$.

which were produced by elastic electron-electron scattering in the target. This kind of background which gave some troubles in distinguishing wide angle bremsstrahlung events has been extensively investigated and will be discussed in the following.

A range telescope of scintillation counters ($P_1\ P_2\ P_3\ \bar{P}_4$) detects protons emitted in the horizontal plane with kinetic energies between ~ 50 and ~ 100 MeV. Two total-absorption Čerenkov counters (20 cm in diameter, 12 radiation lengths thick, lead glass, 2 m from the target) detect the outgoing electron and photon emitted at the same angle with respect to the incident beam ($\sim 25^{\circ}$) but symmetrically with respect to the horizontal plane (see Fig. 11). The nature of the particle, either electron or photon, is determined by looking at signals from two plastic scintillators placed in front of each Čerenkov counter. The experimental apparatus is symmetrical with respect to the horizontal plane so that kinematically equivalent WAB events ($e\,\gamma\,p$) are defined by the fast logic as:

$$(P_1P_2P_3\bar{P}_4)\ (E_1E_1'C_1)(\bar{E}_2\bar{E}_2'C_2) \qquad \text{or}$$

$$(P_1P_2P_3\bar{P}_4)\ (\bar{E}_1\bar{E}_1'C_1)\ (E_2E_2'C_2)$$

When a master coincidence occurs the pulse height in the two Čerenkov counters was recorded providing the energy of the electron and photon with $\sim 30\%$ resolution (full width at half height); time of flight and pulse amplitude in the counter P_3 (2 cm thick) provided the proton kinetic energy. The accepted phase-space region was determined only by the dimensions of the counters without energy cuts so that the energy spectra of the detected particles can be used as a check "a posteriori" that observed events are really bremsstrahlung events, with no apreciable contamination from other processes.

In Fig. 11 is also shown the apparatus for the elastic electron-proton scattering measurement. The same Čerenkov counters of WAB are used to detect the electron and in addition two auxiliary telescopes to detect the recoil proton. A scattering event is thus defined by the coincidences (S_1S_2) x $(E_2E_2'C_2)$ or $(S_1'S_2')$ x $(E_1E_1'C_1)$.

Besides the WAB events ($e\ \gamma\ p$) also events in which the proton is accompanied by two charged particles, ($e\ e\ p$) events, or by two neutrals, ($\gamma\ \gamma\ p$) events, are recorded. In both cases the only difference with respect to ($e\gamma\ p$) events is due to the nature of the signals from the scintillation counters in front of the Čerenkov counters, pulse amplitudes and time of flight criteria being well met with ($e\gamma\ p$) events.

The only genuine physical process giving ($e\ e\ p$) events is trident production $e^- + p \rightarrow e^- + p + e^+ + e^-$ which, however, is lower by a factor greater than 100, due to cross section and phase space distribution,

with respect to WAB. Actually (e e p) events must be attributed to accidentals of soft electrons from electron-electron scattering in the target and (e γ p) events.

The elastic electron-electron scattering background has been measured as a function of the direction and intensity of the magnetic field surrounding the target. Direct measurements of the accidental rates in the plastic scintillators in front of the Čerenkov counters have also been made. This allows the determination of the two quantities α_1 and α_2, one for each pair of scintillation counters in front of the Čerenkov, which represent the probability that a photon be interpreted as an electron due to accidentals of soft electron.

The determination of the two parameters α_1 and α_2 can however be done in a completely independent way taking advantage of the symmetry of the electrons and photons detecting system. In fact the number of WAB events in which the electron is detected in the Čerenkov above the horizontal plane and the photon in the Čerenkov below the horizontal plane (e γ p) (see Fig. 11) must be equal to the number of events in which the electron is detected below the horizontal plane and the photon above the horizontal plane (γ e p). The assumption that no genuine (e e p) events are produced gives a further condition in determining the parameters α_1 and α_2.

The agreement between the two determinations of α_1 and α_2 that one gets by the two different methods is very good.

Electroproduction of $\pi_s^{o'}$ gave the measured ($\gamma\gamma$ p) events. The background from π^o electroproduction can give two different kind of events; when $q_t^2 > m_\pi^2 = (135\ \mathrm{MeV})^2$ events of the (e γ p) type are expected, a decay photon from a π^o being detected in coincidence with inelastically scattered electron and proton. This kind of event can be distinguished from a genuine WAB event only with very precise measurements of the electron and photon emission angles and of the proton angles and kinetic energy. The emission angle of the bremsstrahlung photon is in fact unequivocally determined by the parameters $T_p\ \theta_p\ \varphi_p\ \theta_e\ \varphi_e$; photons from π^o decay instead are spread over a large fraction of solid angle around the π^o direction ($\pi_s^{o'}$ are emitted nearly in the same direction as the photon of WAB). This kind of background, however, does not contribute in the two kinematical situations explored by the experiment since $q_t^2 = (70\ \mathrm{MeV})^2$, $q_t^2 = (100\ \mathrm{MeV})^2$. Also, ($\gamma\gamma$ p) events can occur because of π^o electroproduction in the target; in this case the two decay photons from a π^o are detected, the inelastically scattered electron (mainly in the forward direction and with low energy) being missed by the Čerenkov counters. Conversion of a ($\gamma\gamma$ p) event into a WAB event (e γ p) can then occur because of an accidental with soft electrons from elastic e - e scattering so that a subtraction has to be applied.

The two parameters α_1 and α_2 account also for this effect in the actual separation of bremsstrahlung events.

The true counting rates of $(e\ e\ p)_t$, $(\gamma\gamma p)_t$, $(e\gamma p)_t$, $(\gamma\ e\ p)_t$ events can in fact be obtained from the measured using the following relations

(17a) $$(\gamma\gamma p)_m = (\gamma\gamma p)_t(1-\alpha_1)(1-\alpha_2)$$

(17b) $$(e\gamma p)_m = (e\gamma p)_t(1-\alpha_2)+(\gamma\gamma p)_t(1-\alpha_2)\alpha_1$$

(17c) $$(\gamma\, e\, p)_m = (\gamma e p)_t(1-\alpha_1) + (\gamma\gamma p)_t(1-\alpha_1)\alpha_2$$

(17d) $$(e\, e\, p)_m = (e\, e\, p)_t + \alpha_2(e\gamma p)_t + \alpha_1(\gamma\, e\, p)_t + \alpha_1\alpha_2(\gamma\gamma p)_t$$

In Fig. 12 is shown the typical behaviour of the quantities defined by equations 17. The condition $(e\gamma p)_t = (\gamma e p)_t$ allows one to obtain α_1 as a function of α_2 by the eq. (17b, c) (straight line $(e\gamma p)_t = (\gamma e p)_t$ Fig. 12. When values of α_1 and α_2 lying on the straight line $(e\gamma p)_t = (\gamma e p)_t$ are taken one is able to calculate the true number of $(e\, e\, p)_t$ events and the total bremsstrahlung rate $(e\gamma p + \gamma e p)_t$ as a function, for example, of α_2. The further condition $(e\, e\, p)_t = 0$ allows one to determine the pair of α_1 and α_2 values which are effective in the actual measurement and thus the real number of WAB events which were measured.

The pair of values of α_1 and α_2 that one gets by this technique is in very good agreement with the values of α_1 and α_2 obtained by direct accidental rates measurements. Further, the total number of WAB events depends slowly, at least in the two kinematical situations explored by the experiment, on the actual values of α_1 and α_2 (see Fig. 12).

In Fig. 13 the spectra of the relevant kinematical quantities as measured by the apparatus are shown. The measured spectra are compared with those expected on the basis of the requirements on the detection angles by integrating the Bethe-Heitler[25] cross section over the accepted phase-space region (Monte Carlo calculation); effects of target length and experimental resolution were accounted for. The regions of q_s^2 and q_t^2 explored in the two kinematical situations chosen for the experiment are also shown in Fig. 13.

The results are summarized in Table I. The measured cross section is compared to the theoretical cross section $d\sigma_{BH}$[25] calculated to lowest order in e^2 including proton form factors (column 7). To evaluate the WAB cross section including proton recoil, the "scaling law" $G_E(q^2) = G_M(q^2)/\mu$ and the dipole fit $G_E(q^2) = (1 - (q^2/0.71\ GeV^2))^{-2}$, which reproduce well the experimental values of G_E and G_M in the range of q^2 involved ($q^2 \simeq 3\ f^{-2}$), were used.

In column 8 the experimental cross section is compared with the theoretical one $d\sigma_{BH+C}$ including virtual Compton contribution. The vir

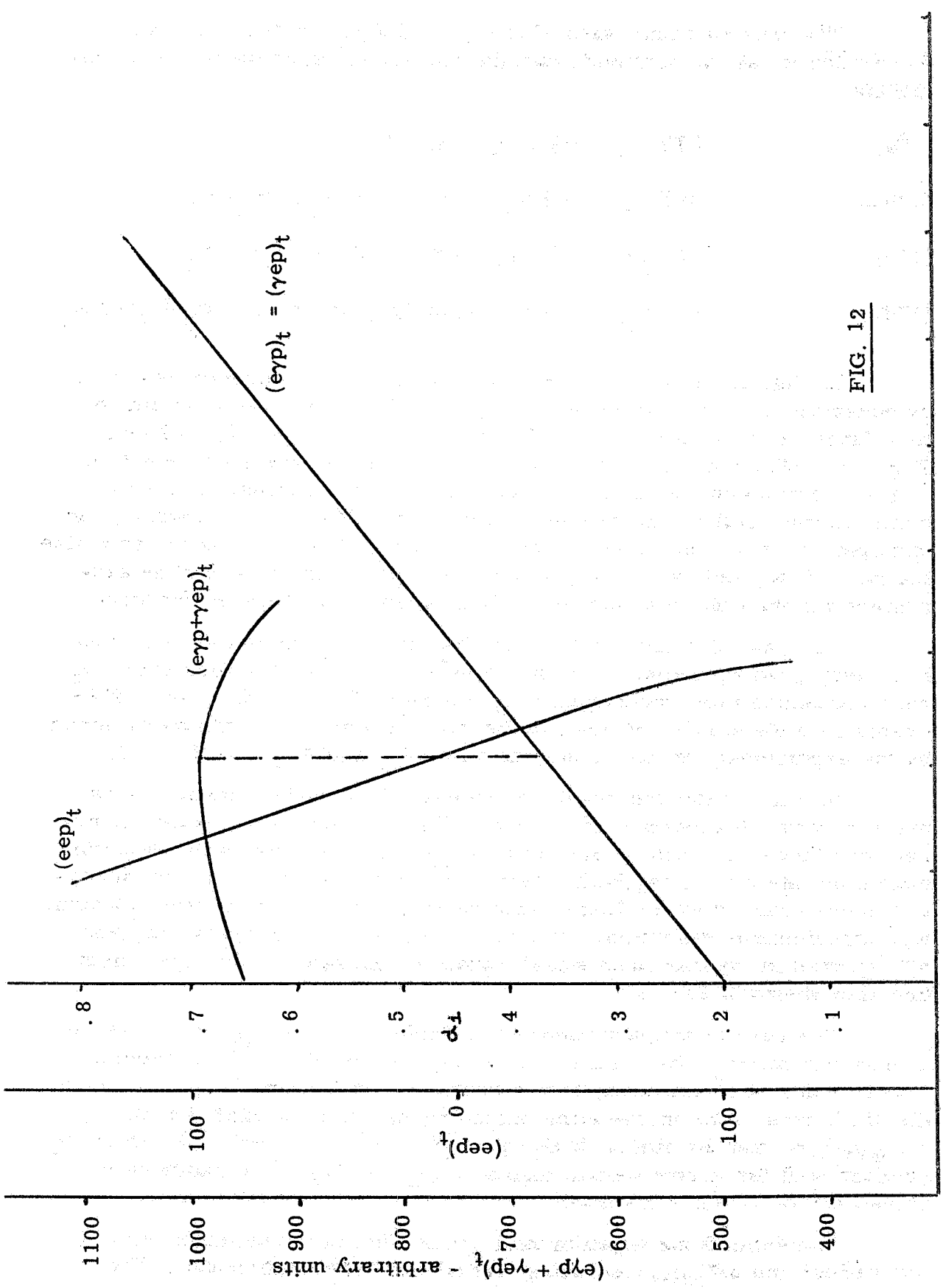
(eγp + γep)$_t$ - arbitrary units
1100
1000
900
800
700
600
500
400
100
0
100
(eep)$_t$
.8
.7
.6
.5
.4
.3
.2
.1
d_1
0
.1
.2
.3
.4
.5
.6
.7
.8
.9
d_2
(eep)$_t$
(eγp+γep)$_t$
(eγp)$_t$ = (γep)$_t$

FIG. 12

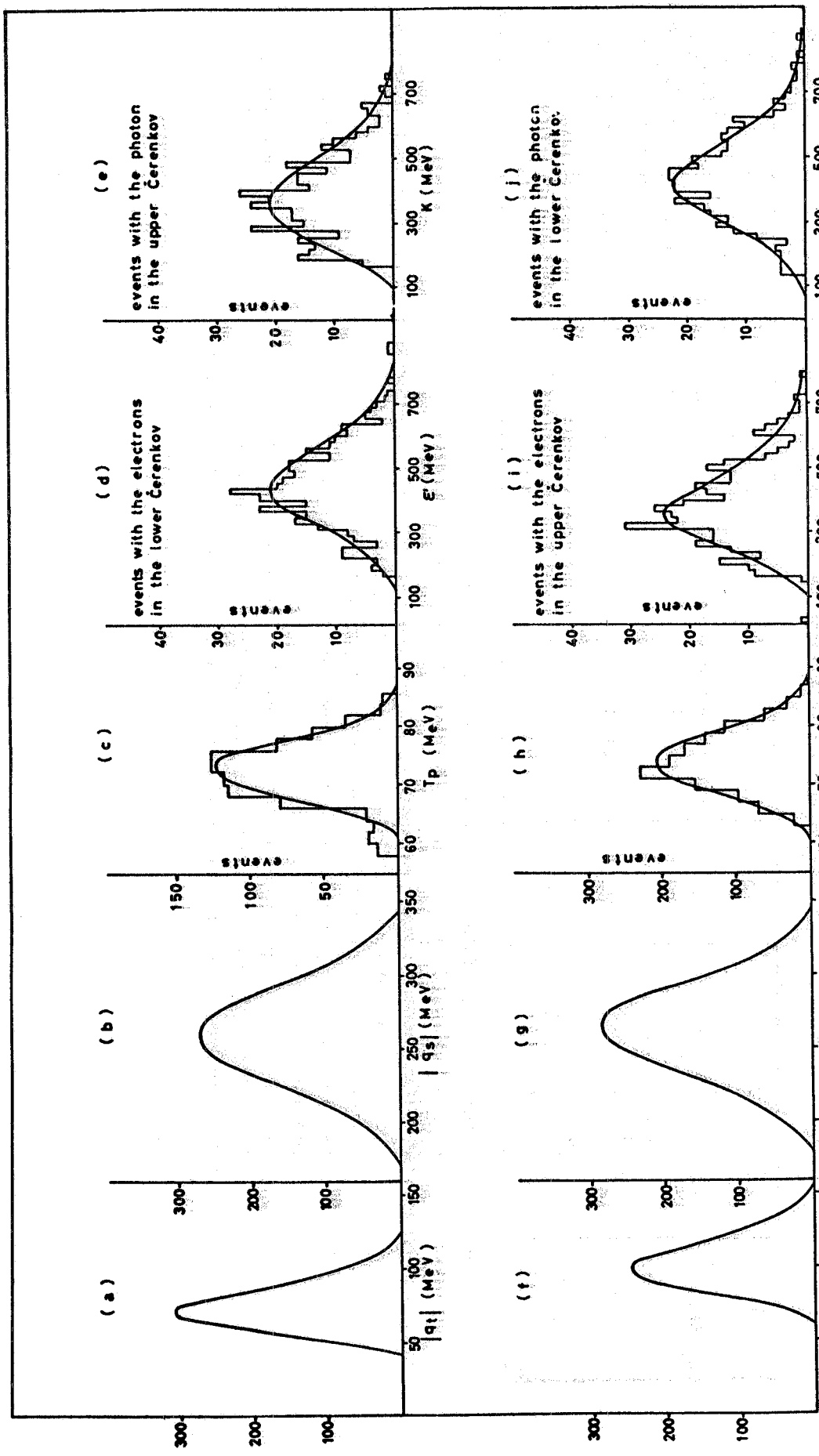

FIG. 13 - Spectra of the relevant kinematical parameters, as obtained from Monte Carlo calculations, including experimental acceptance and resolution (full line). For comparison with the theoretical prediction, we show in (c) (d) (e) (h) (i) (j) the measured spectra relative to a sample of the events. Tp, ε', k are the kinetic energy of the emitted proton, the energy of the emitted electron and photon respectively.

TABLE I - SUMMARY OF RESULTS

1	2	3	4	5	6	7	8	9
$q_t^2(\text{MeV})^2$	$q_s^2(\text{MeV})^2$	$T_p(\text{MeV})$	$\mathcal{E}(\text{MeV})$	uncorrected events	corrected events	$\frac{d\sigma_{exp}}{d\sigma_{BH}}$	$\frac{d\sigma_{exp}}{d\sigma_{BH+C}}$	$(\frac{d\sigma_{exp}}{d\sigma_{th}})_{scatt}$
$(70)^2$	$(260)^2$	74	900	1872	2083	$.995 \pm .04$	$.955 \pm .04$	$.935 \pm .04$
$(100)^2$	$(265)^2$	74	900	1282	1130	$1.065 \pm .05$	$.993 \pm .05$	$.995 \pm .03$

col. 1, 2 : mass squared of electron propagators (see Figg. 10a, 13).
col. 3 : central value of the proton kinetic energy spectrum (see Fig. 13).
col. 4 : incident electron beam energy.
col. 5 : number of measured WAB events $(e\gamma p + \gamma ep)_m$.
col. 6 : number of corrected WAB events $(e\gamma p + \gamma ep)_t$ (see text).
col. 7 : ratio between experimental WAB cross section and theoretical Bethe-Heitler cross section including proton form factors.
col. 8 : ratio between experimental WAB cross section and theoretical Bethe-Heitler cross section including proton form factors and virtual Compton contribution.
col. 9 : ratio between the experimental scattering cross section and the theoretical one.

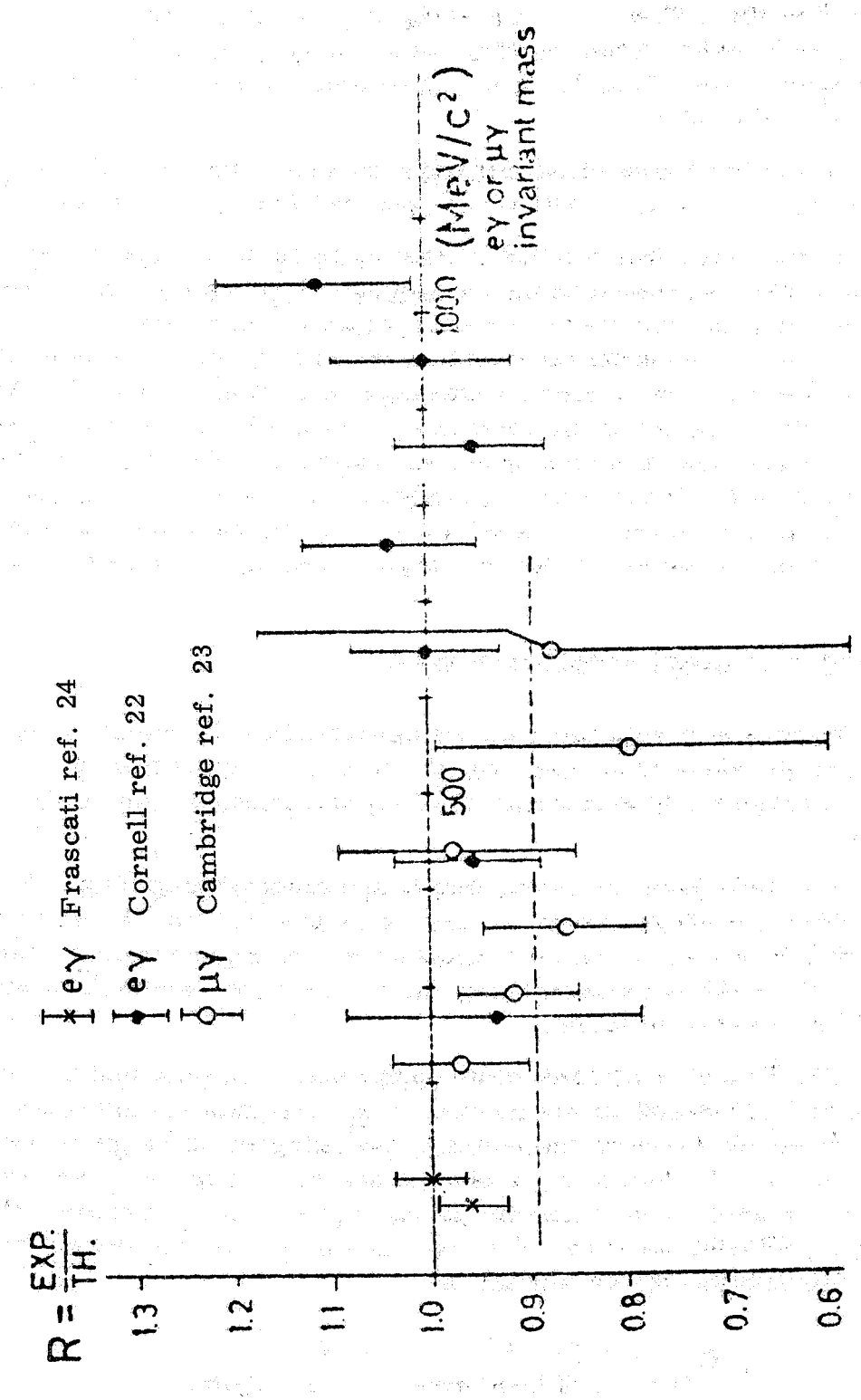
R = EXP./TH.
1.3
1.2
1.1
1.0
0.9
0.8
0.7
0.6
500
1000 (MeV/c²)
eγ or μγ
invariant mass
eγ Frascati ref. 24
eγ Cornell ref. 22
μγ Cambridge ref. 23

FIG. 14

tual Compton amplitude cannot be estimated from quantum electrodynamics alone since it depends on hadron couplings and can involve resonant intermediate states. The virtual Compton contribution has been evaluated according to M. Greco, A. Tenore and A. Verganelakis[26] who take into account both the virtual proton and the first isobar effects. The contamination from virtual Compton effect depends quite strongly on the kinematical configuration of the WAB measurement; in particular it is increasing as q_t^2 increases.

In the two kinematical situation explored the virtual Compton contribution is $\sim$ 4% at $q_t^2 = (70\ \text{MeV})^2$ and $\sim$ 7% at $q_t^2 = (100\ \text{MeV})^2$.

In the last column of table I the results on the elastic electron-proton scattering measurement are given. The agreement between the measured and the theoretical cross section is considered to be very satisfactory since the scattering counting rate is much more sensitive to the geometry of the experimental apparatus than is that of WAB; (in particular to the primary beam alignement, to the length of the H_2 target (20 cm) and to the angular acceptances of counters). These effects have been accounted for in the Monte Carlo calculation performed to evaluate the expected scattering cross section. Radiative corrections have been applied to the scattering cross section although they are negligible in this case ($\sim$ 1%)

RADIATIVE CORRECTIONS FOR WAB.

Radiative corrections for bremsstrahlung to lowest order in e^2 are due to two different processes which involve the emission of real photons and the emission and reabsorption of virtual photons (loop diagrams) see Fig. 15.

The first process is the double bremsstrahlung (Fig. 15a) whose contribution is mainly due to the emission of soft photons; when the energy of one of the mitted photons is less than the experimental energy resolution ΔE double bremsstrahlung can not be experimentally distinguished from single bremsstrahlung.

The double bremsstrahlung contribution is obtained by integrating the wholly differential cross section in the two photons energies over the energy of one of the emitted photons, the integration range being extended from zero to ΔE. Actually, a divergence occurs in the lower integration limit. As is well known this kind of divergence can be parametrized by attributing a fictitious mass λ to the photon so that the double bremsstrahlung cross section can be written as

$$\sigma_{DB} = \sigma_{DB\ \text{infrared}}(\lambda) + \sigma_{DB\ \text{finite}}$$

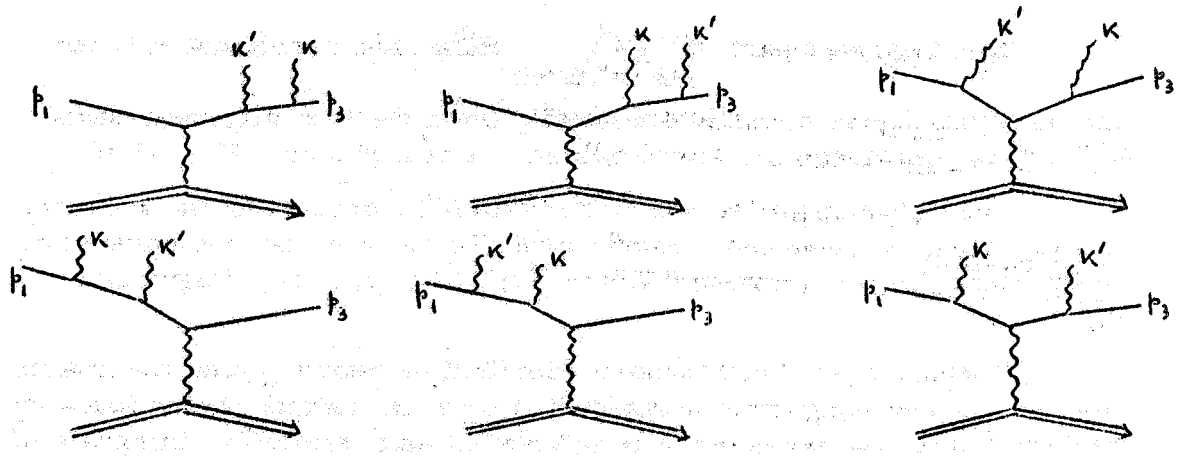

FIG. 15 a) - Double Bremsstrahlung.

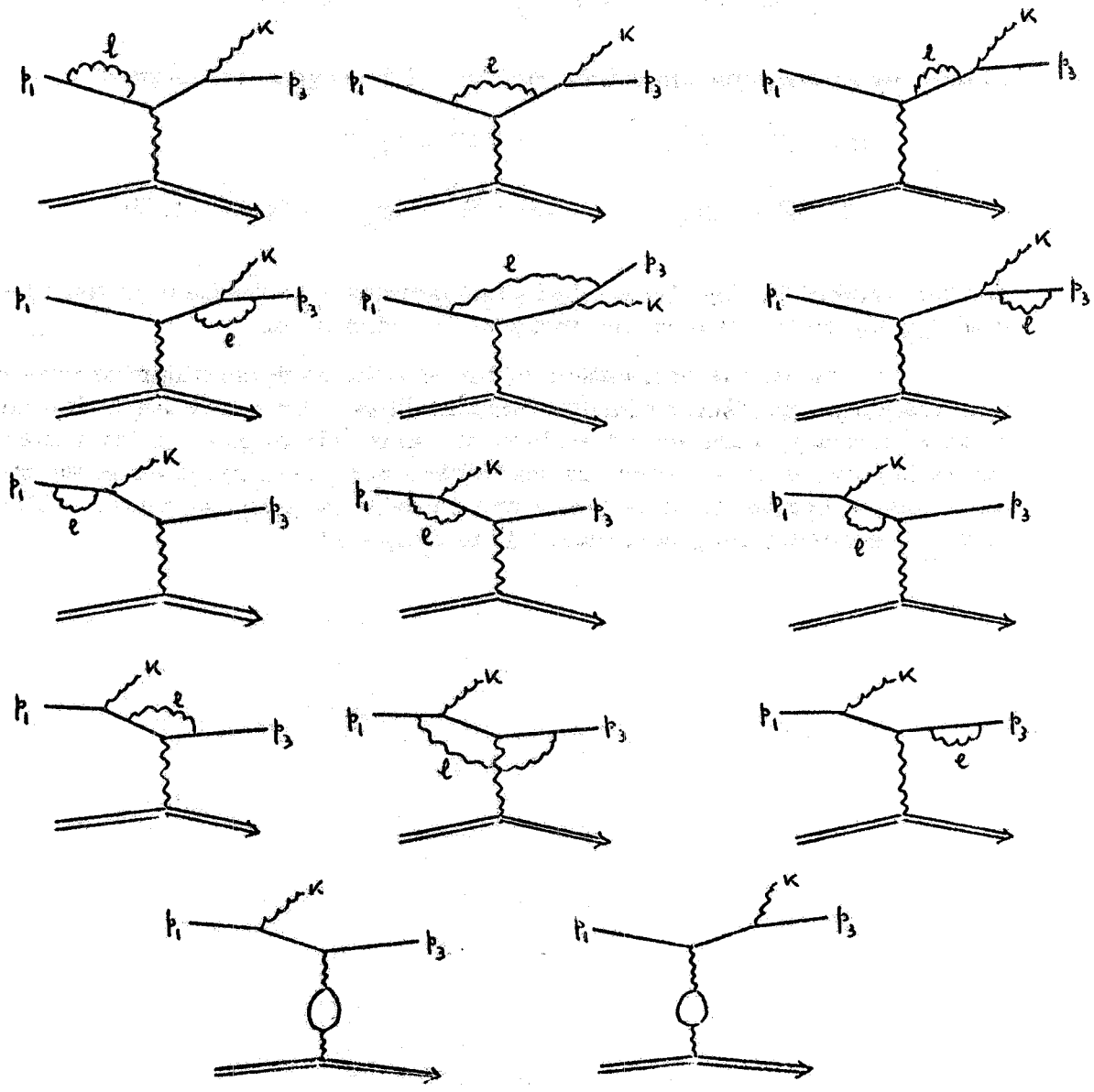

FIG. 15 b) - Loop diagrams.

The divergent part $\sigma_{DB\ infrared}(\lambda)$ must then cancel out with the analogous divergent contribution arising from the loop diagrams which involve the emission and reabsorption of virtual photons (Fig. 15 b).

The virtual photons contribution must be accounted for in evaluating radiative corrections to lowest order because of the interference between Bethe-Heitler (bremsstrahlung Fig. 10 a) and loop diagrams of Fig. 15 b.

Evaluation of virtual photon contribution requires that the matrix elements of loop diagrams be integrated over the virtual photon four-momentum 1 from the mass-shell to infinity so that, typically, integrals of the following form must be calculated

$$J_{(1,\sigma,\sigma\tau,\sigma\tau\varsigma)} = \int d^4 1 \frac{(1, 1_\sigma, 1_\sigma 1_\tau, 1_\sigma 1_\tau 1_\varsigma)}{(0)(1)(2)(3)}$$

where, as an example (notations of Fig. 15 b have been adopted)

$$(0) = (1^2 + \lambda^2) \qquad (1) = (1^2 - 2p_1 \cdot 1)$$

$$(2) = (1^2 - 2p_3 \cdot 1) \qquad (3) = (1^2 + 2p_3 \cdot k - 2p_3 \cdot 1 - 2k \cdot 1)$$

and the symbol $(1, 1_\sigma, 1_\sigma 1_\tau, 1_\sigma 1_\tau 1_\varsigma)$ denotes 1 in the case of the integral J_1, 1_σ in the case of the integral J_σ, and so on.

At present the calculation of the interference contribution between loop diagrams and Bethe-Heitler diagrams has been performed; this calculation has been carried out without any approximations, in particular terms depending on the electron mass have been retained so that the results can be applied to analogous experiments involving μ mesons. The double bremsstrahlung calculation is in progress.

BIBLIOGRAFIA. -

(1) - C. Bernardini, Internal Report LNF-68/42 (1968).
(2) - V. Silvestrini, Internal Report LNF-68/17 (1968).
(3) - A.I. Akhiezer and V.B. Berestetskii, Quantum Electrodynamics (Interscience, 1965).
(4) - J.C. Ward, Phys. Rev. 78, 182 (1950); Y. Takahashi, Nuovo Cimento 6, 371 (1957).
(5) - J.A. McClure and S.D. Drell, Nuovo Cimento 37, 1638 (1965).
(6) - N.P. Chang and M.S. Mani, Phys. Rev. 134, B896 (1964).
(7) - N.M. Kroll, Nuovo Cimento 45, A65 (1966).
(8) - H. Lehmann, Nuovo Cimento 11, 342 (1954).
(9) - A.M. Bincer, Phys. Rev. 118, 855 (1960).
(10) - T.D. Lee and G.C. Wick, Columbia University Preprint.
(11) - A.F. Grillo, Internal Report LNF-69/1 (1969).
(12) - G. Charpak, F.J.M. Farley, R.L. Garwin, T. Muller, J.C. Sens and A. Zichichi, Nuovo Cimento 37, 1241 (1965); F.J.M. Farley, J. Bailey, R..C.A. Brown, M. Giesh, M. Jöstlein, S. Van der Meer, E. Picasso and M. Tannenbaun, Nuovo Cimento 45, 281 (1966); D.T. Wilkinson and H.R. Crane, Phys. Rev. 130, 852 (1962); W.H. Lousille, R.W. Pidd and H.R. Crane, Phys. Rev. 94, 7 (1954); J. Bailey, W. Bartl, G. Von Bochmann, R.C.A. Brown, F.J.M. Farley, H. Jostlein, E. Picasso and R.W. Williams, Phys. Letters 28B, 287 (1968); A. Rich, Phys. Rev. Letters 20, 967, 1221 (1968); Proc. Lund Intern. Conf. on Elementary Particles, (1969).
(13) - R. Gatto, Proc. Intern. Symp. on Electron and Photon Interactions at High Energies, Hamburg (1965), vol. I, pag. 106.
(14) - W.C. Barber, B. Gittelman, G.K. O'Neill and B. Richter, Phys. Rev. Letters 16, 1127 (1966); Intern. Conf. on High-Energy Phys. Vienna (1968).
(15) - J.E. Augustin, J. Buon, B. Delcourt, J. Haissinski, J. Jeanjean, D. Lalanne, M. Nguyen Ngoc, J. Perez-Y-Jorba, F. Richard, F. Rumpf and D. Treille, Proc. 4th Intern. Symp. on Electron and Photon Interaction at High Energies, Daresbury (1969).
(16) - S.A. Colgate and F.C. Gilbert, Phys. Rev. 89, 790 (1953); E. Malamud and R. Weill, Nuovo Cimento 27, 418 (1963); F. Fabiani, M. Fidecaro, G. Finocchiaro, G. Giacomelli, D. Harting, N.H. Lipman and G. Torelli, Nuovo Cimento 25, 635 (1962); A. Brown and J. Pine, Nuovo Cimento 27, 850 (1963); P.L. Braccini, I.X. Ion, A. Stefanini, G. Torelli and R. Torelli Tosi, Nuovo Cimento 29, 1215 (1963).
(17) - C. Bacci, R. Baldini-Celio, G. Capon, G.P. Murtas, C. Pellegrini, G. Penso, A. Reale, G. Salvini and M. Spinetti, Proc.

Intern. Symp. on Electron and Positron Storage Rings, Saclay (1967).

(18) - WAEP: B. Richter, Phys. Rev. Letters 1, 114 (1958); R.B. Blumenthal, D.C. Ehn, W.L. Faissler, P.M. Joseph, L.J. Lanzerotti, F.M. Pipkin and G.D. Stairs, Phys. Rev. 144, 1199 (1966); E. Silverman, C. Sinclair and R. Talman, Phys. Rev. Letters 18, 425 (1967); J.G. Asbury, W.K. Bertram, U. Becker, P. Joose, M. Rohde, A.J.S. Smith, S. Friedlander, C.L. Jordan and S.C.C. Ting, Phys. Rev. 161, 1344 (1967); M. Alvensleben, U. Becker, W.K. Bertram, M. Binkley, K. Cohen, C.L. Jordan, T.M. Knasel, R. Marshall, D.J. Qinn, R. Rhode, G.M. Sanders and S.C.C. Ting, Phys. Rev. Letters 21, 1501 (1968).

(19) - WAMP; A. Alberigi-Quaranta, M. De Pretis, G. Marini, A. Odian, G. Stoppini and L. Tau, Phys. Rev. Letters 9, 226 (1962); J.K. De Pagter, A. Boyarski, G. Glass, J.I. Friedman, H.W. Kendall, M. Gettner, J.F. Larrabern and R. Weinstein, Phys. Rev. Letters 12, 739 (1964); J.K. De Pagter, J.I. Friedman, G. Glass, R.C. Chase, M. Gettner, E. Von Goeler, R. Weinstein and A.M. Boyarski, Phys. Rev. Letters 17, 767 (1966); D.J. Quinn and D.M. Ritson, Phys. Rev. Letters 20, 890 (1968); S. Mayes, R. Imlay, P.M. Joseph, A.S. Keizer, J. Knowles and P.C. Stein, Phys. Rev. Letters 22, 113 (1969).

(20) - F.E. Low, Phys. Rev. Letters 14, 238 (1965).

(21) - C. Betournè, H. Nguyen Ngoc, J. Perez-y-Jorba and J. Tran Thanh Van, Phys. Rev. Letters 17, 70 (1965); H.J. Beherend, F.W. Brasse, J. Engler, E. Ganssauge, H. Hultschig, S. Galster, G. Hartwig and H. Shopper, Phys. Rev. Letters 15, 900 (1965); C.D. Boley, J.E. Elias, J.I. Friedman, G.C. Hartmann, H.W. Kendall, P.N. Kirk, M.R. Sogard, L.P. Van Speybroek and J.K. De Pagter, Phys. Rev. 167, 1275 (1968); S. Barshay and A. Franklin, Phys. Rev. 160, 1294 (1967).

(22) - R.M. Siemann, W.W. Ash, K. Berkelman, D.L. Hartill, C.A. Lichtenstein and R.M. Littuaer, Phys. Rev. Letters 22, 421 (1969); Internal Report Cornell, CLNS-90 (1969).

(23) - A.D. Liberman, C.M. Hoffman, E. Engels, Jr., D.C. Imrie, P.G. Innocenti, R. Wilson, C. Zajde, W.A. Blanpied, D.G. Stairs and D.J. Drickey, Phys. Rev. Letters 22, 663 (1969).

(24) - C. Bernardini, F. Felicetti, R. Querzoli, V. Silvestrini, G. Vignola, L. Meneghetti, S. Vitale and G. Penso, Lettere al Nuovo Cimento 1, 15 (1969).

(25) - P.S. Isaev and I.S. Zlatev, Nuovo Cimento 13, 1 (1959); R.A. Berg and C.N. Lindner, Phys. Rev. 112, 2072 (1958); A. Costescu and T. Vescan, Nuovo Cimento 48 A, 1041 (1967).

(26) - M. Greco, A. Tenore and A. Verganelakis, Phys. Letters 27 B, 317 (1968); Nuovo Cimento 58 A, 743 (1968).